CHAPTER 4

Genetic differentiation in experimental *Drosophila melanogaster* metapopulations III - Local extinction and recolonization

with F. J. WEISSING and R. BIJLSMA

ABSTRACT

In contrast with the large body of theory predicting the dynamics of genetic variation and differentiation in idealized metapopulations, experimental studies aiming to validate these models are mostly limited to unstructured populations. We evaluated experimental *Drosophila melanogaster* metapopulations of increasing complexity by varying the levels and patterns of gene flow. The present study focuses on the consequences of population turnover, *i.e.*, local extinction and recolonization of demes. We examine the difference between migrant-pool and stepping-stone migration, the robustness of results based on replication and the consequences for population fitness and tolerance to external stress factors.

Population turnover increased stochasticity at the metapopulation level, resulting in a more rapid loss of diversity and higher levels of differentiation than without local extinction. Therefore, effective metapopulation sizes decreased much faster in the presence than in the absence of population turnover. Despite striving for constant environmental conditions, migration and colonization rates fluctuated considerably between generations, resulting in high to very high variation among replicates when population turnover occurred regularly. The migration configurations showed several differences resulting mainly from the higher cost of migrant-pool migration, although none were significant due to the high variation among replicates. Assessments of population fitness and stress tolerance both showed substantial interdemic variation, indicating that the distribution of genetic variation in a metapopulation can become very uneven when population turnover occurs regularly.

Although replicated experimental metapopulations provide an excellent means to validate theory because they allow standardization, our study also points out some limitations. Logistic constraints (one marker locus, few demes, few replicates) substantially increase the already considerable variation due to population turnover. Relaxing experimental standardization even a little may result in large deviations from theoretical predictions, which will undoubtedly be larger yet for complex natural systems.

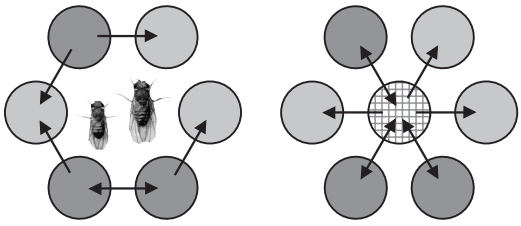

INTRODUCTION

In conservation genetic studies, both the genetic diversity within and the genetic differentiation among demes in a metapopulation are often used to assess its prospects of survival, and to infer recommendations for its future management (*e.g.*, Keyghobadi *et al.* 2005). Local extinction and subsequent recolonization events correspond to genetic bottlenecks for single demes because colonists may be few in number, and may be closely related. Homozygosity may increase rapidly in such newly colonized demes, which will potentially lead to a fitness reduction due to the expression of recessive deleterious alleles (Saccheri *et al.* 1998, Crnokrak & Roff 1999, Bijlsma *et al.* 2000, Hedrick & Kalinowski 2000, Keller & Waller 2002, Reed *et al.* 2003b, Armbruster & Reed 2005, Reed 2005), although increased homozygosity may also stimulate the purging of (highly) deleterious alleles in small populations (Wang *et al.* 1999, Miller & Hedrick 2001, Crnokrak & Barrett 2002, Glemin 2003). Moreover, genetic diversity may be lost due to genetic drift, which may in turn affect the potential of a local population to adapt to changing environmental conditions (Montgomery *et al.* 2000, England *et al.* 2003).

In the last three decades, much theory on the genetic consequences of population fragmentation has been developed. Slatkin (1977) presented the first theoretical study analyzing the effects of local extinction and colonization on the autozygosity (*i.e.*, the probability that two alleles chosen at random within a population are identical by descent) in a metapopulation with gene flow occurring in line with Wright's (1951) classical island model of migration. Slatkin's study introduces two types of island model: the "continent-island" model (model I) assuming that all migrants originate from an infinite source population outside the focal metapopulation of n finite demes, and the "finite-island" model (model II) assuming that all migrants originate from within the metapopulation. A further distinction is made between two models of colonization: the "propagule-pool" model where all colonists founding a particular population originate from a single source and the "migrant-pool" model where the colonists founding a particular population represent a random selection from all migrating individuals in the metapopulation. Neither model includes local demography, but assumes that the constant, maximum deme size N is achieved immediately after colonization (Slatkin 1977). Wade & McCauley (1988) reformulated Slatkin's results by equating autozygosity to F_{ST} (*i.e.*, the standardized variance of allele frequencies) in a system receiving genetically unrelated migrants (Rousset 2004, see also the appendix in CHAPTER 3). They showed that the equilibrium value $\hat{F}_{ST}$ in both models I and II tends to become very similar if the number of demes n is large ($n > 20$). For both models, differentiation increases with extinction rate e under the propagule-pool model of colonization. Under the migrant-pool model, however, differentiation may either increase or decrease depending on the number of colonists k relative to the number of migrants Nm. F_{ST} tends to increase with e when $k < 2Nm$, but to decrease when $k > 2Nm$. These findings were later generalized in a series of theoretical contributions (*e.g.*, by considering various patterns of genetic structure in the group of colonists, Whitlock & McCauley 1990, Pannell & Charlesworth 1999). While theory is fairly well developed for the

various island models of migration, there are relatively few studies on the consequences of stepping-stone migration. Moreover, these studies either exclude local extinction (Maruyama 1970a, b) or migration among extant demes (Maruyama & Kimura 1980).

In contrast to the large body of theory, the number of experimental studies aiming at validating the theoretical models is limited. Recent studies include *e.g.*, the long-term observation of genetic structure in relatively simple natural metapopulations with population turnover (Haag *et al.* 2002, 2005, 2006), or the investigation of the consequences of genetic bottlenecks in a laboratory setting (Reed *et al.* 2002, 2003a). However, a common disadvantage of natural populations is the limited possibility for standardization and replication, whereas the use of experimental populations not embedded in a metapopulation context may not allow for extrapolation to natural metapopulations. Our study aims to extend the replicated experimental approach to a metapopulation context.

We investigate the consequences of population fragmentation and population turnover, with population turnover defined as the local extinction of demes followed by recolonization from the remaining extant demes in either the same or subsequent generations. We monitor the changes of genetic diversity and differentiation based on an eye colour polymorphism in standardized and replicated laboratory *Drosophila* metapopulations, and we compare our findings with expectations based on theoretical models. These experiments closely match and complement our earlier studies focusing on the effects of genetic drift in small isolated populations (CHAPTER 2) and migration between such populations (CHAPTER 3). These studies provided baseline values for metapopulations with constant deme sizes and migration rates in the absence of population turnover. In the current study we allow deme sizes and migration rates to fluctuate, and we include pre-scheduled local extinction events in half of the replicate metapopulations.

To place our experimental results in a more general perspective, we perform individual-based computer simulations that mimic the setup of our experiments. The simulations allow us to predict average patterns of diversity and differentiation and the corresponding levels of variation based on many "*in silico*" replicates, whereas the number of experimental replicates is limited by logistic and time constraints.

We focus on the effect of population turnover on the patterns of genetic diversity and differentiation, addressing three aspects in particular: (i) the effect of spatial configuration (*i.e.*, migration following either a migrant-pool or a stepping-stone pattern), (ii) the consistency of results based on replicate metapopulations, and (iii) the consequences of fragmentation and population turnover for population fitness and tolerance to external stress factors.

Migrant-pool migration where migrants spread globally over the entire metapopulation is generally expected to counteract genetic drift more efficiently than stepping-stone migration where migrants can only make steps of one deme per generation. Hence, we expect that genetic differentiation among demes will happen more slowly in case of migrant-pool migration. In the presence of local extinction, theory predicts that the emerging pattern of genetic differentiation will strongly reflect the relative magnitudes of extinction and migration rates, the number of colonists relative to typical deme sizes,

and the origin of the colonists (Hedrick & Gilpin 1997). All these processes are stochastic in nature, which will likely induce relatively much variation between metapopulations. Local extinction at a high rate may result in many demes being extinct at the same time, which might in turn cause a genetic bottleneck at the metapopulation level. Genetic bottlenecks and a subsequent decrease of the effective metapopulation size might affect population fitness negatively through inbreeding depression and the loss of allelic diversity due to genetic drift, although purging of deleterious alleles may mitigate the decrease of fitness to some extent (Wang & Caballero 1999, Rousset 2003, Gaggiotti & Hanski 2004). Since the effects of purging can be already ambiguous in case of undivided small populations, it is unclear what we might expect in a metapopulation context.

MATERIAL AND METHODS

DROSOPHILA STOCKS

We used the same mutant *Drosophila melanogaster* lines as in our previous study (for a detailed descriptions of these stocks, see CHAPTER 2). The alleles *bw* and bw^{75} at the *brown* locus (II-104.5) in combination with the mutation *scarlet* (III-44) in homozygous condition result in distinct eye colours for the three genotypes at the *bw* locus. Homozygous *bw*//*bw* individuals have white eyes, homozygous bw^{75}//bw^{75} individuals have red-brown eyes, and heterozygous bw^{75}//*bw* individuals have intermediate orange eyes at 25°C. All fly stocks are raised in 125 ml bottles on 30 ml of standard medium (26 g dead yeast, 54 g sugar, 17 g agar, and 13 ml nipagine solution (10 g nipagine in 100 ml 96% alcohol) per liter) with antibiotics (250 mg streptomycin per liter), and under standard conditions at 25°C, 40-60% RH and 24 hours of light. In the experiments, small fly populations were raised on 18 ml of standard medium without antibiotics in 40 ml glass vials under standard conditions. We anaesthetized the flies with CO_2 before handling.

EXPERIMENTAL SETUP

The experimental setup included two different spatial configurations of fragmented populations (metapopulations), each consisting of six demes represented by compartments connected through two plastic 4 mm Ø tubes that could be closed or opened with a small tap (fig. 4.1A). Each compartment held a 40 ml glass vial with 18 ml medium and about 50 flies. The spatial configurations enabled migration according to either an equidistant *n*-island setup, or a circular bidirectional stepping-stone setup. In the *n*-island setup (fig. 4.1B) migrants originating from many small demes ("islands") congregate in a migrant pool and then distribute with equal probabilities to arrive at any deme including their own source population. Hence, in the experimental *n*-island configuration all six demes are connected to a seventh, central compartment ("migrant pool") that all migrants have to pass through before they can move into another deme. The central compartment contained a vial with medium to attract flies in a similar way as populated demes, but it was closed at the top with nylon wire mesh to avoid actual colonization. In

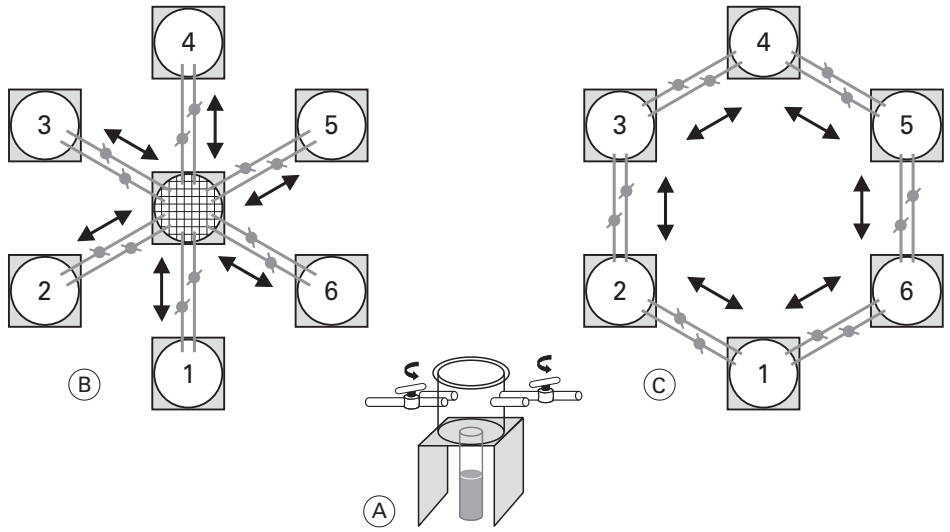

Figure 4.1. Setup of experimental *Drosophila melanogaster* metapopulations in two spatial configurations. A metapopulation consists of six demes represented by compartments (A) connected through tubes that can be opened or closed for migration by taps. Each deme is either connected to all other demes via a central compartment (B) representing a migrant pool, or connected directly to two adjacent demes (C) in a circular stepping-stone pattern. A compartment is populated with a vial containing medium and a fly population, whereas the central compartment in configuration (B) holds a vial containing only medium that is closed on top by a piece of nylon wire mesh. With the taps open, migrating flies can move to and fro through the tubes as indicated by the arrows.

the bidirectional stepping-stone setup (fig. 4.1C) migrants have a large probability to arrive in either one of two adjacent demes, and much smaller probabilities to end up in demes that are more than one step away. In the corresponding stepping-stone configuration the demes are connected to each other on two sides in a circular pattern, so that migrants can both leave and enter in two directions. Due to the presence of the central compartment in the migrant-pool configuration the physical distance between two demes is twice as long as in the stepping-stone configuration and includes an enforced stop in the middle. Hence, the migration rate in the stepping-stone configuration might be higher than in the migrant-pool configuration.

We used six replicate metapopulations for each spatial configuration, and 12 undivided control populations without gene flow. One metapopulation (= replicate) consisted of six demes (= 40 ml glass vials with 18 ml medium) with on average 50 founding individuals per deme in each generation. Ideally, the unfragmented control populations (= 125 ml standard bottles) should have been initiated with 6 x 50 = 300 individuals, but due to experimental limitations they comprised 210 founding individuals per generation on average. Note that the average numbers are harmonic means because the census sizes fluctuated over generations. For each spatial configuration we looked into the effects of local extinction events and subsequent colonizations through

migration. Hence, in three of six replicate metapopulations local extinction of one or more demes occurred according to a pre-defined schedule (see next section), and three metapopulations were used as control populations with migration but without extinction. Thus, this setup resulted in four different experimental series with three replicates each: (i) migration in a migrant-pool configuration with local extinction (replicates MPX1, MPX2 and MPX3), (ii) migration in a migrant-pool configuration without extinction (replicates MP1, MP2 and MP3), (iii) migration in a stepping-stone configuration with local extinction (replicates SSX1, SSX2 and SSX3), and (iv) migration in a stepping-stone configuration without extinction (replicates SS1, SS2 and SS3). The local extinction events for each replicate metapopulation in the extinction series MPX and SSX were assigned *a priori* by randomly allotting extinction events to individual demes with probability $e = 0.1$ per deme for each generation. Note that the three metapopulations within each series are not exact replicates, because the predefined extinction schedules were different for each metapopulation.

EXPERIMENTAL PROCEDURE

All experimental series started without any initial genetic differentiation ($F_{ST} = 0$) with 100% heterozygous orange-eyed individuals collected from the mixed F1 of $bw^{75}//bw^{75}$ x $bw//bw$ parents and the reciprocal crossing $bw//bw$ x $bw^{75}//bw^{75}$. The flies were reared in glass vials that were placed in the matching compartments of the corresponding migration appliances (fig. 4.1) on day 14 of each generation to enable migration. Depending on the activity of the flies that fluctuated considerably from generation to generation, the taps were opened for 12-24 hours aiming at one migrant per deme on average (the duration interval was estimated from different levels of fly activity in previous migration tests for both appliances, data not shown). Since we only controlled duration but no other aspects of migration, migrants might be either females or males, and the majority had likely mated before migration. During migration we placed each appliance under its own circular lamp (Philips Fluotone TL-E Pro 32W/840, dimmed to 45% of its maximum intensity) in a climate room where central lights were turned off to avoid any bias from phototaxis in migration behaviour (Shorrocks 1972). We monitored allele frequencies and heterozygosities (after migration), and the occurrence of extinction and colonization events over 40 generations for each replicate.

Generations did not overlap and took 14 days to develop. One experimental generation consisted of the following six stages. (i) Several hundreds of eggs were laid per vial, and to avoid severe crowding we limited this amount in two successive stages. We cut the layer of food with newly-laid eggs into four pieces and divided these over four new vials. This procedure provided us with one new experimental population and three emergency backup populations. (ii) After pupation we removed any excess offspring, so that about 50 pupae per vial were left. (iii) After eclosion we allowed the flies a few days for maturing and mating, and then we placed the vials in the corresponding appliances and opened the taps for migration. (iv) Extinction happened at this stage just before migration: offspring in a deme destined to go extinct in generation t were scored for that generation, but were not allowed to migrate any more. Instead, we placed vials with

medium of the same quality as in the populated vials but without flies in all empty patches in the appliance to allow for colonization. Thus, extinction and colonization may occur in the same generation. (v) After the allotted migration period (see above) we closed the taps, and we removed all flies from the compartments and transferred them to fresh vials to start the next generation. In this stage we scored the number, sex and genotypes of colonists for all empty patches, and also of any flies that were left in the central compartment of the migrant-pool configuration (fig. 4.1B) after migration. Since these flies were discarded from the experiment, they represent a cost of migration in the migrant-pool configuration. (vi) After egg-laying for 2-3 days all parental flies were frozen and stored to score genotype frequencies at a later time.

ASSESSMENT OF REALIZED MIGRATION RATES

Based on pilot migration tests in both appliances we expected that on average one individual per deme would migrate, corresponding to a migration rate $m = 1/N = 0.02$ for an average deme size $N = 50$. Although we did not monitor the migration process exactly we can estimate the realized migration rates in both appliances retrospectively from the numbers of colonists M_C in n_E empty demes that we did monitor exactly for all metapopulations with local extinction. Most theoretical models do not distinguish between immigration (*i.e.*, the average number of individuals moving into a new deme per generation) and emigration (*i.e.*, the average number of individuals leaving a source deme per generation) because both quantities are equal if all demes are occupied each generation. In our experimental systems, however, extinct demes tended to stay empty for several generations resulting in fewer occupied demes n_O on average than the total number of $n = 6$ demes. Hence, we expect that the emigration rate m_E will be higher than the immigration rate m_I in most cases because fewer demes are available for emigration than for immigration (*i.e.*, $n_O m_E = 6m_I$). To estimate m_I and m_E, we assume that the probability to enter an empty deme is equal to the probability to enter an occupied deme. The average number of colonists per empty deme, $m_C \,/\, n_E$, can then be used to estimate the average number of immigrants per deme $Nm_I = m_C \,/\, n_E$, and to infer the average number of emigrants per deme as $Nm_E = 6M_C \,/\, n_O m_E$.

In the migrant-pool configuration several migrants M_E were usually still in the central compartment when we closed the taps. Hence, the average number of emigrants per deme is given by $Nm_E = (6M_C \,/\, n_E + M_E) \,/\, n_O$. The difference between both expressions of Nm_E indicates the "cost of migration" in the migrant-pool configuration.

ASSESSMENT OF FITNESS AND STRESS TOLERANCE

In generation 35, we evaluated the average fitness and the tolerance to external stress factors of each metapopulation. To infer the average fitness of a metapopulation we measured the net fecundity of females and the egg-to-adult viability under standard conditions. We calculated the net fecundity (*i.e.*, the average number of viable offspring per female) from the number of offspring of five breeding pairs raised under standard conditions in one 23 ml plastic vial on 9 ml of standard medium with antibiotics (100 mg ampicillin per liter). We collected the breeding pairs as virgins and allowed them to mate

and lay eggs for 15 days with transfers to a fresh vial every third day, resulting in five consecutive series of offspring. We counted the total number of offspring in all five series and translated these numbers into an average value per female that was corrected for females escaped during transfer, but not for dead ones. Thus, the net fecundity measure corresponds to the product of female fecundity (= number of eggs laid), offspring viability (= egg-to-adult survival) and adult female survival, and assumes no limiting effects of male fitness traits. In this way, we estimated the net fecundity of a deme as the average of five samples per deme (*i.e.*, 6 x 5 = 30 samples per metapopulation), and the net fecundity of a bottle control population as the average of 30 samples per bottle.

We estimated egg-to-adult viability as the fraction of adult individuals eclosing from 300 eggs that were randomly sampled and were raised either under standard conditions or under stress conditions. We kept females for 4-6 hours in a small container placed upside down with a thin layer of medium on the lid and some fresh yeast to stimulate egg-laying. After removal of the females we carefully picked the eggs from the medium on the lids and placed them in 23 ml plastic vials on 9 ml of the required medium. To avoid crowding we used six vials with 50 eggs per vial for each sample of 300 eggs. We inferred the viability per deme for all metapopulations from samples of 300 eggs per deme, and the viabilities of all bottle control populations from a sample of 300 eggs per bottle.

To assess the stress tolerance in a metapopulation we measured the viability for two environmental stress factors (high temperature, high ethanol concentration in the food medium) and the resistance to starvation of males. We determined the viability of eggs raised on standard medium at 29°C, 40-60% RH and 24 hours of light to assess the effect of high temperature, and the viability of eggs raised on medium with ethanol added in a concentration of 12.5% at standard conditions to assess the effect of high ethanol concentrations. For comparison between treatments, we used stress tolerance $T_S = V_S / V_C$, *i.e.*, the egg-to-adult viability V_S under stress conditions relative to the viability V_C under control conditions.

We estimated starvation resistance from the LT50 (*i.e.*, the median time to death of the tested individuals) of 10 newly eclosed virgin males kept in vials containing 9 ml agar medium only. We checked the vials daily until the first death occurred, and from that moment we scored the numbers of dead males three times per twenty-four hours until all flies had died, using the midpoint of the 8-hour interval where death occurred as an estimate of the time of death. We determined the LT50 of five replicates for each deme in a metapopulation and for each bottle control population. Because we did not have enough flies in all cases to start all five replicates of a deme/bottle at the same time, we used the arithmetic mean of the five replicates to estimate the LT50 of the deme/bottle rather than determining the overall LT50 of 5 x 10 = 50 males.

F-STATISTICS AND EFFECTIVE METAPOPULATION SIZE

For each generation we used the genotype frequencies per deme to infer the allele frequencies and the expected heterozygosity H_S. We then used these heterozygosities to calculate the fixation index $F_{ST} = (H_T - \bar{H}_S)/H_T$ for each metapopulation, where H_T is

the expected heterozygosity of the metapopulation calculated from the average allele frequencies, and $\bar{H}_S$ is the average expected heterozygosity of a deme (Hartl & Clark 1997). We also calculated a higher level, global fixation index $F_{TG} = (H_G - \bar{H}_T)/H_G$ for each series of three replicate metapopulations, with H_G the expected heterozygosity of the cluster of metapopulations, and $\bar{H}_T$ the average expected heterozygosity of a single metapopulation. The index F_{TG} represents the differentiation among metapopulations, *i.e.*, the variation among replicates.

To view our experimental results in light of the general theoretical models, we compared the observed F_{ST} with theoretically predicted equilibrium values, assuming that F_{ST} approximates its equilibrium value in the midrange of the experiment (*i.e.*, generations 15 to 25). Whitlock and McCauley (1990) showed that for a continent-island (model I) metapopulation in equilibrium and with an infinite number of demes, $\hat{F}_{ST}$ can be approximated by:

$$\hat{F}_{ST} = \frac{1 + Ne/k}{1 + 4Nm + 2Ne[1 - \varphi(1 - 1/2k)]} \quad , \tag{4.1}$$

where N is deme size, m is the migration rate, e is the extinction rate, k is the number of colonists, and φ is the probability of common origin, *i.e.*, the probability that two randomly chosen alleles in a group of colonists originate from the same source. In a later study, Pannell and Charlesworth (1999) showed that this approximation also holds for a finite-island (model II) metapopulation with migrant-pool colonization ($\varphi = 0$) when the number of demes n is sufficiently large and e is of the same magnitude as m and k/N. We will discuss the consequences of a small number of demes for this approximation later. In the absence of extinction ($e = 0$), eqn (4.1) reduces to Wright's (1951) well-known approximation $\hat{F}_{ST} = 1/(1 + 4Nm)$.

The effective size of a metapopulation is often used as a measure of the loss of genetic variation. We use the observed F_{ST} to infer the effective size of the experimental metapopulations. The effective metapopulation size is defined as the size of an idealized, undivided Wright-Fisher population that would show the same dynamics of variation in allele frequency changes as the actual metapopulation (reviewed in Wang & Caballero 1999). Whitlock and Barton (1997) proposed a general expression for the effective metapopulation size N_e^M:

$$N_e^M = \frac{nN}{1 - F_{ST} + V[1 + F_{ST}(2N - 1)n/(n - 1)]} \quad , \tag{4.2}$$

where n is the number of demes and V represents the variance in reproductive success among demes. When all demes contribute equally to the next generation through migration, this variance is zero, and eqn (4.2) reduces to $N_e^M = nN/(1 - F_{ST})$. According to Whitlock and Barton (1997), the variance in reproductive success among demes is $V = e/(1 - e)$ for a metapopulation with local extinction at rate e and subsequent recolonization within the same generation.

When applying the above equations, we replace deme size N by the effective deme size $N_e \approx 0.56N$ to compensate for the lottery polygyny mating system of *Drosophila melanogaster* (CHAPTER 2), and we use the actual number of occupied demes n_O instead of n because recolonization occurred generally not within the same generation. We further assume that all demes contribute equally in the absence of local extinction, using the harmonic mean to estimate the average census deme size $N = 50$ over time. Hence, we set $V = 0$ and the effective deme size $N_e = 0.56N = 28$ in equation (4.2). In the presence of population turnover we assume variable contributions of demes with $V = e/(1 - e)$ and $e = 0.1$. Finally, we estimate the effective size of a hypothetical undivided population with a census size equal to the census size of the metapopulations ($N = 6 \times 50 = 300$) as $N_e = 0.56N = 168$.

In addition, we infer the variance and eigenvalue effective metapopulation sizes based on linear regression independent of F_{ST} (CHAPTER 2). The variance effective size is estimated from linear regression of the variance in allele frequency change within the metapopulation between two successive generations as a function of the allele frequency in the parental generation ($\sigma^2_{\delta p} = p(1 - p)/2\hat{N}^M_e$). Similarly, the eigenvalue effective size is estimated from linear regression of the change in heterozygosity between two successive generations as a function of the heterozygosity of the parental generation ($\Delta H = H/2\hat{N}^M_e$).

COMPUTER SIMULATIONS AND PARAMETERS

The aim of using individual-based simulations is twofold. First, the simulations allow us to place the experimental results in a theoretical perspective. They can be used to derive expectations and matching confidence limits that allow detecting significant deviations of the experimental results from various null hypotheses. Second, the simulations allow extrapolating our findings beyond the observed patterns emerging from known variables, *e.g.*, by introducing a multiple locus approach (see the discussion section).

The simulations take account of the lottery polygyny mating system (males can mate with more than one female) that is typical for *Drosophila melanogaster* (Bateman 1948), of differences in fecundity among females, and of directional selection for the (red) bw^{75}-allele that occurred in the experimental fly stocks (CHAPTER 2). Extinction is typically implemented as an event occurring at random with probability e per deme per generation. We also generated *in silico* replicates for each of our metapopulations by imposing extinction schedules identical to those in the experimental metapopulations. However, since the results from these simulations were almost identical to the results of simulations based on the average extinction rate for both configurations, we have not explored this option further. The simulations take no account of intra-deme demography, hence colonized demes grow to size N in one generation similar to the assumption of the theoretical models.

For all simulations, generations are discrete, the mating system is lottery polygyny with remating and the population size and genetic parameters (one locus, two alleles, no mutation) are kept constant. Based on our earlier experiments (CHAPTERS 2 and 3) we assume that the remating probability is $\rho = 0.2$ and that the variance-to-mean ratio of offspring contributed to the next generation is $\alpha = 1.6$. For a given migration rate m, the

number of emigrants per deme is drawn from a Poisson distribution with mean = Nm. The migrant's sex is allotted at random with a probability of 0.5 for each sex, and we assume that migrants have mated before migration. The extra mortality during migration in the migrant-pool configuration is not implemented in the simulations.

Although this study focuses on the interplay of drift, migration and local extinction in the absence of selection, we include selection in the standard simulations because its effect appeared to be substantial in our previous study. Given the bias in favour of the bw^{75}-allele that we found in all previous experiments, we expect that this is the case in our current experiments as well. Hence, we implement viability selection through an additive model with selection coefficient s and relative viabilities of 1, $1 - s/2$ and $1 - s$ for the three genotypes $bw^{75}//bw^{75}$, $bw^{75}//bw$ and $bw//bw$, respectively. Based on the estimates obtained in our previous study where we found that selection coefficients depended on population size (CHAPTER 2), we used selection coefficients $s = 0.12$ for the vial populations and $s = 0.18$ for the bottle populations in the current experiment. Deviations from the standard parameterization indicated above are explained in the appropriate sections.

STATISTICAL ANALYSIS

As in our previous studies, we mostly used simulations for the statistical analysis of the data by constructing 95% confidence ranges from the 2.5 and 97.5 percentiles of 1000 simulation runs, with each run representing one replicate metapopulation. In addition, we calculated the average of three replicates (as for each of our experimental scenarios) that were drawn randomly from the 1000 simulation runs. Repeating this procedure 1000 times resulted in a new dataset of average values that we used to construct the corresponding 95% confidence ranges.

To test the results of the fitness and stress tolerance assessments for differences between groups (*i.e.*, metapopulations with migration and with or without local extinction, and unfragmented control populations) we used a non-parametric Kruskal-Wallis test (Statistix 8.0) with Bonferroni correction for the number of tests.

RESULTS

MIGRATION, EXTINCTION AND COLONIZATION RATES

We intended to set up a small system with relatively few demes, a high extinction rate, and a colonization rate of the same order of magnitude as the extinction rate to ensure sufficient genetic dynamics within relatively few generations. We first evaluate how closely the realized migration, extinction and colonization rates (table 4.1) match the intended setup.

Although it was not possible to quantify migration by direct observation for logistic reasons, we had the impression that migration regularly happened at either higher or lower rates than expected. This variation was probably related to external, (micro-)environmental factors, since migration activity seemed to be correlated among the replicates

Table 4.1. Extinction, migration and colonization in experimental metapopulations with migrant-pool (MPX) and stepping-stone (SSX) migration. The realized extinction rate is the probability that an extant deme did go extinct per generation. The number of extant demes is the harmonic mean over generations. The realized numbers of emigrants and immigrants are the average numbers per deme inferred from the observed numbers of colonists in empty demes. The gross colonization rate is the probability of migrants moving into an empty deme regardless of their subsequent reproductive success, whereas the net colonization rate is the probability of a successful colonization event (*i.e.*, founding a viable population in an empty deme). The last column shows the average number of founders per successful colonization event. Unless indicated otherwise, averages are arithmetic means with standard errors in brackets.

meta population	realized extinction rate e	extant demes n_O	emigrants per extant deme Nm_E	immigrants per deme Nm_I	gross colonization rate c^*	net colonization rate c	number of colonists k
MPX1	0.133	2.54	0.90 (0.34)	0.56 (0.22)	0.133	0.092	2.55 (1.39)
MPX2	0.068	4.62	0.92 (0.27)	0.63 (0.18)	0.347	0.224	2.09 (0.50)
MPX3	0.062	3.36	0.43 (0.24)	0.23 (0.12)	0.050	0.021	3.00 (3.48)
MPX	0.088 (0.023)	3.72	0.75 (0.16)	0.47 (0.12)	0.211 (0.068)	0.127 (0.050)	2.55 (0.26)
SSX1	0.121	2.99	1.79 (0.63)	0.86 (0.31)	0.250	0.111	5.17 (1.94)
SSX2	0.094	4.11	0.95 (0.22)	0.60 (0.15)	0.300	0.217	1.92 (0.38)
SSX3	0.111	4.75	3.14 (0.65)	2.39 (0.55)	0.595	0.500	3.48 (0.57)
SSX	0.109 (0.012)	4.15	1.96 (0.64)	1.28 (0.56)	0.382 (0.108)	0.276 (0.116)	3.52 (0.94)

running in parallel. The consequences of this variation, however, differed between replicates, since at any given time the replicates differed in the number of vacant demes. Accordingly, temporal variation in migration activity resulted in variation between metapopulations.

Extinction in both configurations was planned *a priori* with a probability $e = 0.1$ per deme per generation. However, we found during the experiment that extinct demes did not become colonized for several generations (figs. 4.2 and 4.3), presumably reflecting the large variation in migration activity between generations. The average number of extant demes (tab. 4.1) is therefore considerably lower than the total number of demes $n = 6$, and the realized extinction rates (*i.e.*, the extinction probability of an extant deme per generation) per metapopulation turned out to be more variable than planned (tab. 4.1). In the migrant-pool configuration (fig. 4.2) we cancelled planned extinction events in replicates MPX1 (simultaneous extinction of demes 4 and 5 in generation 14) and MPX3 (simultaneous extinction of demes 1 and 3 in generation 37) to avoid metapopulation extinction (and thus loss of a replicate before the end of the experiment). This reduced the extinction probability for the migrant-pool configuration to $e = 0.09$ on average.

We inferred the migration rates for both experimental configurations retrospectively as indicated in the methods section. The realized numbers of emigrants Nm_E (tab. 4.1) were mostly close to or larger than the planned number of one migrant per deme

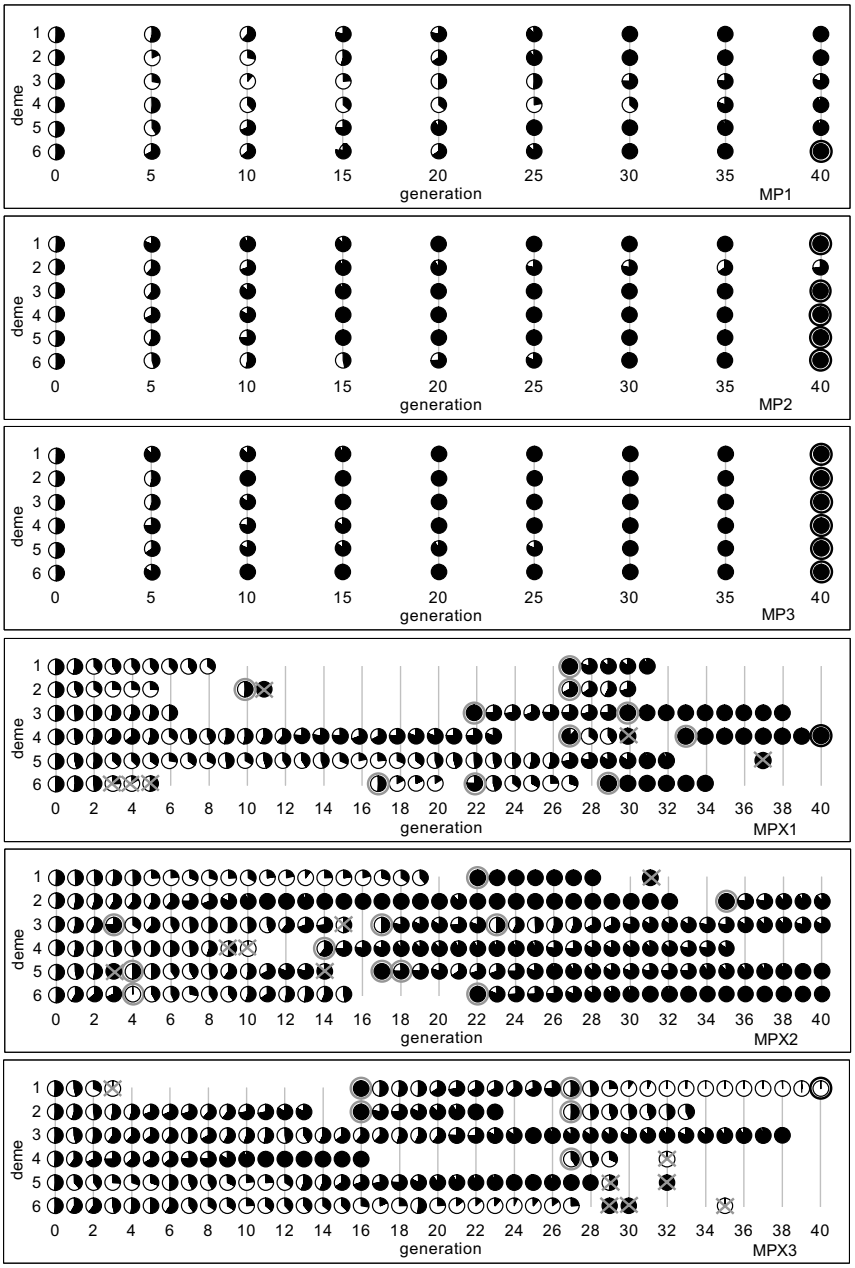

Figure 4.2. Allele frequencies in *D. melanogaster* metapopulations with migrant-pool migration, and in the absence (replicates MP1, 2 and 3) or presence (replicates MPX1, 2 and 3) of local extinction and recolonization. Markers indicate the frequencies of the bw^{75}-allele (black) and the *bw*-allele (white) in each of the six demes in a metapopulation over 40 generations. Empty slots indicate extinct demes. Grey outlines or crosses at a marker indicate successful or unsuccessful (*i.e.*, immigration without founding) colonization, respectively. Black outlines indicate fixation for either eye colour allele in generation 40.

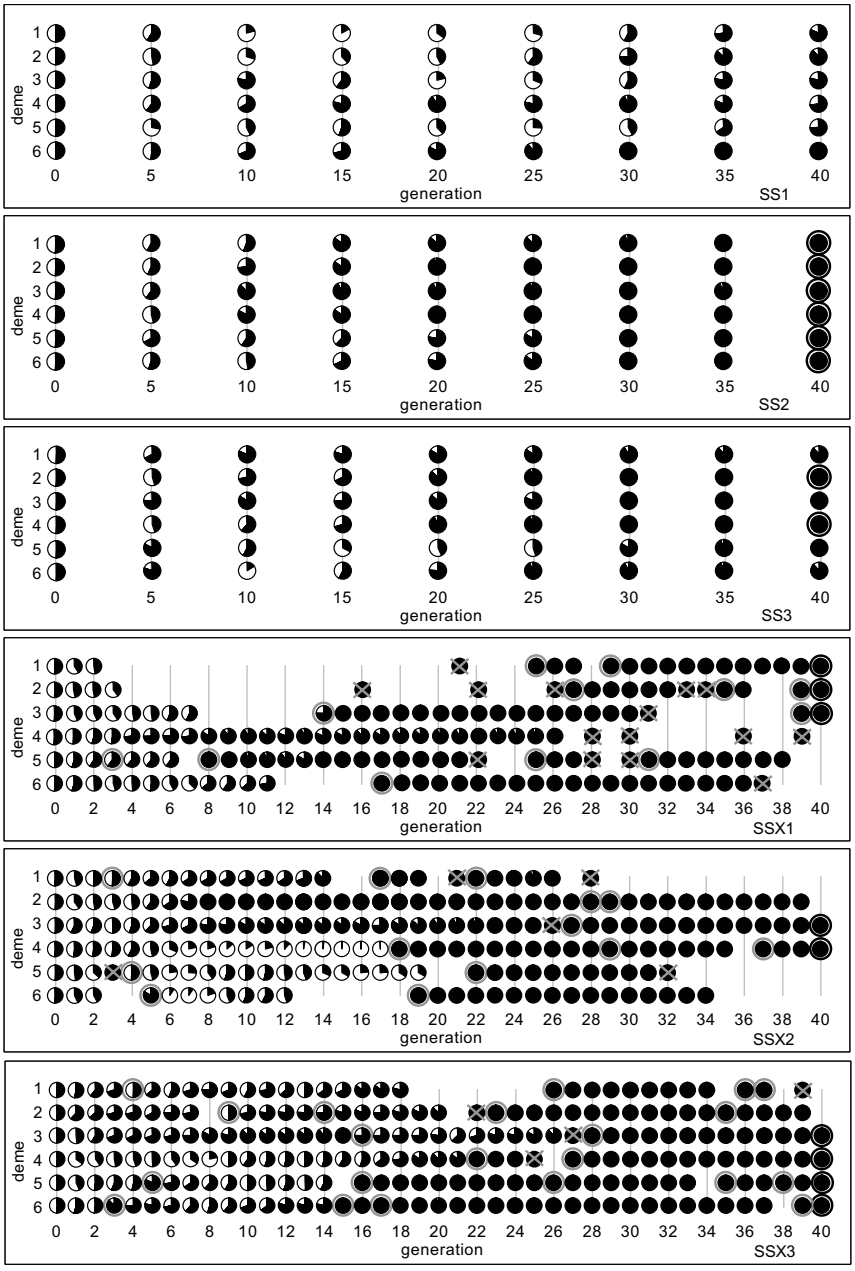

Figure 4.3. Allele frequencies per deme in *D. melanogaster* metapopulations with stepping-stone migration, and in the absence (replicates SS1, 2 and 3) or presence (replicates SSX1, 2 and 3) of local extinction and recolonization. Symbols as in fig. 4.2.

whereas the numbers of immigrants Nm_I are generally lower, although the variation among replicate metapopulations is considerable. Both emigration and immigration tended to be substantially lower in the migrant-pool configuration (MPX) than in the stepping-stone configuration (SSX), but these differences were not significant due to the large variation among the replicates within each configuration.

The gross colonization rates c^* (*i.e.*, all events of migrants arriving in an empty deme regardless of the subsequent founding success, tab. 4.1) indicate that empty demes were populated by migrants at an equal or higher rate than extant demes going extinct on average. However, not every colonization event resulted in a new viable population (figs. 4.2 and 4.3, grey circles *versus* crosses). Hence, although the net colonization rate c (*i.e.*, the probability of colonization followed by the founding of a viable population, tab. 4.1) was considerably higher than the extinction rate on average (tab. 4.1) this was not the case for three individual metapopulations (MPX1, MPX3 and SSX1) due to the large variation in colonization rates. Thus, individual metapopulations may run a high risk of extinction although the condition for metapopulation persistence ($c > e$) is met on average (figs. 4.2 and 4.3).

The average number of individuals per successful colonization event k (tab. 4.1) varied considerably both between and within metapopulations, probably again as a consequence of the large variation in migration activity. In spite of the relatively large numbers of colonists, 63% and 37% of the colonization events were due to single mated females in the migrant-pool and stepping-stone configuration, respectively. In contrast, individual-based simulations predict about 30% colonizations by single mated females on average for both configurations.

For the planned experimental setup, individual-based simulations predict an extinction probability of 7.5% (about 75 of 1000 metapopulations are lost before generation 40) for both configurations. In contrast, 50% (3 out of 6) of our metapopulations would have gone extinct within 40 generations without intervention. The above results suggest that the large variation in migration activity between generations and the resulting low colonization success caused the high observed extinction probability.

GENETIC DIVERSITY AND DIFFERENTIATION

We will now focus on the evolution of genetic diversity within demes and genetic differentiation among demes within metapopulations. Figure 4.2 (migrant-pool migration) and figure 4.3 (stepping-stone migration) show the changes of the allele frequencies at the *bw*-locus within individual demes. In figure 4.4 we compare the average allele frequencies in the metapopulations with the allele frequencies in the undivided bottle populations. Figure 4.5 shows the average expected heterozygosity $\bar{H}_S$ as a measure of the average genetic diversity within demes for each replicate metapopulation, and the average of three metapopulations to picture the global trend for each series. Figure 4.6 shows similar plots of the fixation index F_{ST} as a measure of the genetic differentiation among demes.

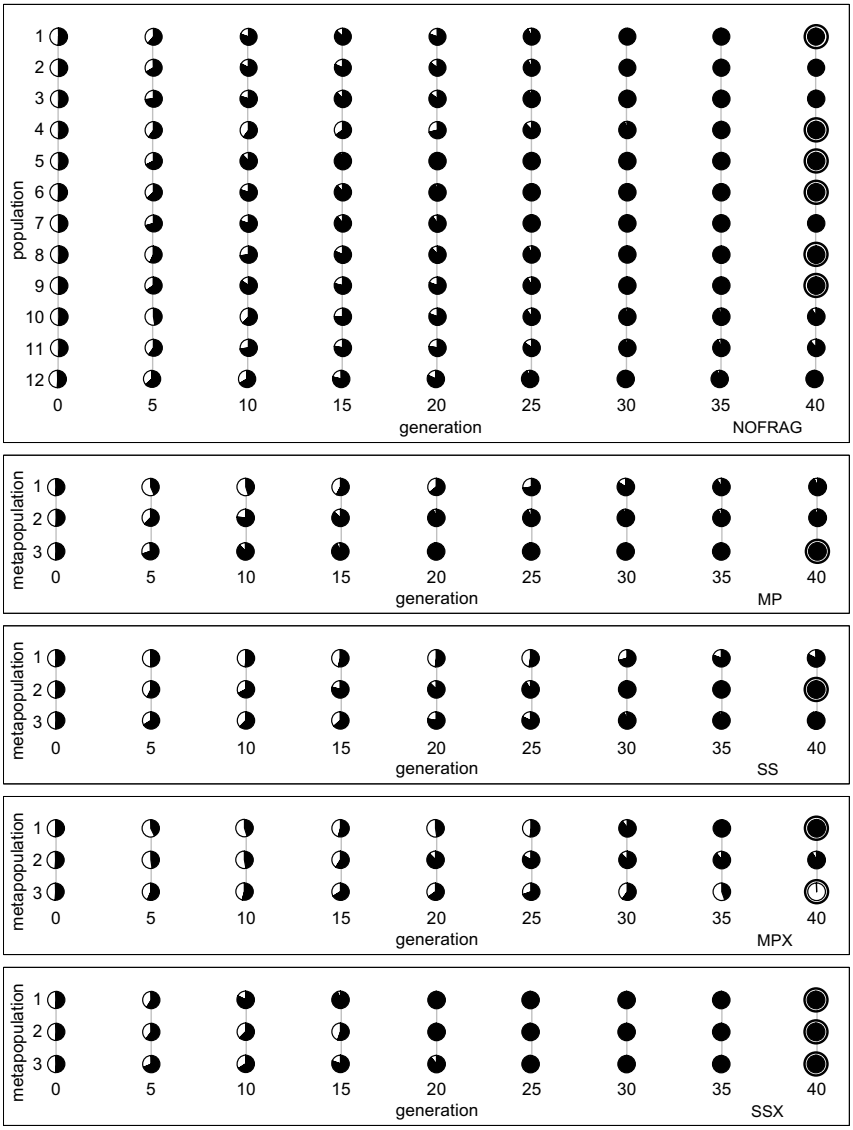

Figure 4.4. Allele frequencies in unfragmented *D. melanogaster* populations (NOFRAG), and average allele frequencies in metapopulations with either migrant-pool or stepping-stone migration, in the absence (MP & SS) or presence (MPX & SSX) of local extinction and recolonization. Symbols as in fig. 4.2.

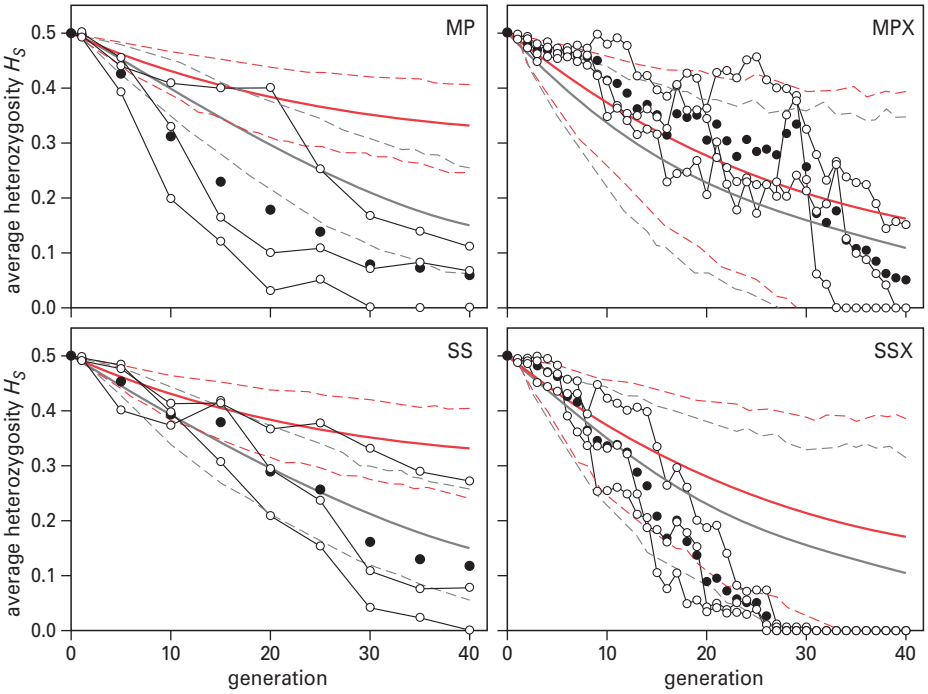

Figure 4.5. Observed and predicted genetic diversity in metapopulations with migrant-pool (top) and stepping-stone (bottom) migration, in the absence (left) or presence (right) of local extinction and recolonization. The plots show the average heterozygosity $\overline{H}_s$ of three replicate metapopulations (white circles) and their average (black circles), and predictions from individual-based simulations without (red lines) and with (grey lines) directional selection ($s = 0.12$). Dotted lines indicate 95% confidence bands for the average of three replicate metapopulations.

MIGRANT-POOL *VERSUS* STEPPING-STONE MIGRATION WITHOUT POPULATION TURNOVER

First we evaluate the two migration configurations without extinction and recolonization. At the level of individual demes we find that the bw^{75}-allele approaches fixation within most demes (fig 4.2 series MP & fig. 4.3 series SS), confirming our earlier results that bw^{75} is favoured by selection. In generation 40 half of the demes in the stepping-stone metapopulations and two thirds in the migrant-pool metapopulations are fixed (black outlines). At the metapopulation level, two of the six metapopulations (fig. 4.4 series MP & SS) and six of the 12 large undivided populations (series NOFRAG) are fixed in generation 40. In case of neutral variation, theory predicts a more rapid loss of allelic variation in small, relatively isolated demes than in large random-mixing populations, since the effective population size of a deme is generally much smaller than the effective size of a large population. However, this loss of variation will be different for each deme. As a consequence, more variation will remain in a metapopulation than in an undivided population of equal size. The effective size of a metapopulation is larger

than its census size, hence the loss of variation at the metapopulation level will be slower than in an undivided population of equal census size. Directional selection increases the fixation rate of the favoured allele (Crow & Kimura 1970), and will generally be more effective in a structured population than in an undivided population, especially under the assumption of hard selection (Whitlock 2002). Thus, selection favouring the bw^{75}-allele has presumably been responsible for the observed patterns. Individual-based simulations (data not shown) of undivided populations including selection predict 11% allele fixation after 40 generations, whereas simulations of similar undivided populations without selection predict only 0.1% fixation. Hence, the observed high fixation rates in the bottle populations are plausible.

In the case of neutral variation we expect a slower decline of diversity within demes, but higher levels of differentiation among demes than in the presence of directional selection (Crow & Kimura 1970). Simulations of both migration configurations in the absence (figs 4.5 & 4.6, red lines) and presence (grey lines) of selection confirm these expectations. The simulation results also indicate that the dynamics of migrant-pool and stepping-stone metapopulations are similar when migration rates are equal. The results of the experimental metapopulations, however, show clear differences between both migration configurations (figs 4.5 & 4.6, MP *versus* SS). Although we expect only moderate variation among the relatively small number of replicate metapopulations (*i.e.*, the confidence bands in figs 4.5 & 4.6 indicating the expected variation among three replicates), the loss of genetic diversity in both experimental configurations (fig. 4.5 left) differed (much) more than expected based on the simulations. The average increase of genetic differentiation (fig. 4.6 left) is mostly in line with the prediction from simulations for both configurations for the larger part of the experiment. The sharp decline of differentiation at the end of the experiment, particularly in case of stepping-stone migration, is due to allele fixation at the metapopulation level. Further quantification of the variation among replicate metapopulations by means of the global fixation index F_{TG} measuring genetic differentiation among replicates (data not shown) confirms both trends.

The observed differences between the two migration configurations are presumably the result of the lower migration rate in the migrant-pool than in the stepping-stone configuration (tab. 4.1) due to the larger migration distance and the occasional removal of a number of migrants remaining in the central compartment adding to the cost of migration in the former. Additional factors such as sexual or density-dependant selection or differences in activity due to the light regime (CHAPTER 3) favouring the bw^{75}-allele have probably played a role as well.

LOCAL EXTINCTION AND RECOLONIZATION

Next we look into the effects of local extinction and subsequent recolonization for both migration configurations. The large stochastic effects of extinction and founder events on the allele frequencies of individual demes instantly catch the eye. Allele frequencies may become completely reversed within one generation (fig. 4.3, deme 4 in SSX2), which may eventually even allow fixation of the disadvantageous *bw*-allele at the metapopulation level (fig. 4.2, MPX3). In contrast with the scenarios without local extinction, the

levels of allele fixation in the individual demes differ considerably for the two migration configurations. In case of migrant-pool migration (fig. 4.2, series MPX) fixation happens much slower than in case of stepping-stone migration (fig. 4.3, series SSX). Fixation at the metapopulation level happens more rapid than in both the scenarios without local extinction and the undivided populations (fig. 4.4, NOFRAG). All three stepping-stone metapopulations become fixed within 30 generations although each metapopulation comprises at least three extant demes in most generations. Two of the three migrant-pool metapopulations also become fixed eventually, which in one case is due to the extinction of all but one fixed deme. These results suggest that selection is more efficient in the stepping-stone configuration than in the migrant-pool configuration. Individual-based simulations predict a low level of metapopulation fixation (2.5%) in the absence of population turnover that increases substantially (40%) due to extinction and recolonization for both configurations at equal migration rates. Since effective migration is higher in the stepping-stone setup than in the migrant-pool setup, the resulting selection-drift dynamics may be different for both setups. However, even when we consider the extra cost of migration in the migrant-pool configuration in the simulations (data not shown), the actual fixation rate of the bw^{75}-allele is still higher than predicted in all experimental (meta)populations regardless of the relative differences between hierarchical levels, spatial configurations and migration-extinction scenarios. This confirms our earlier conclusion regarding the probable presence of additional factors favouring the bw^{75}-allele.

The differences between both configurations are reflected in the dynamics of genetic diversity (fig. 4.5 right) and differentiation (fig. 4.6 right). As for the scenarios without local extinction, individual-based simulations predict similar dynamics for both configurations in the absence (red lines) and presence (grey lines) of selection at equal migration rates. In contrast to the scenarios without local extinction resulting in a faster than predicted average loss of diversity (fig. 4.5 left) for both configurations, the decline of diversity (fig. 4.5 right) is faster than predicted by simulations in case of stepping-stone migration (series SSX), but slower than predicted in case of migrant-pool migration (series MPX). The sharp decline of differentiation within the stepping-stone metapopulations (fig. 4.6 right) mirrors the rapid loss of diversity and subsequent allele fixation at the metapopulation level. Both patterns suggest an absolute loss rather than a redistribution of genetic variation.

Quantification of the variation among replicate metapopulations by means of the global fixation index F_{TG} (data not shown) is in line with both the observed high variation and the predicted confidence bands among replicate metapopulations. The, in view of selection favouring the bw^{75}-allele, atypical fixation of the *bw*-allele in metapopulation MPX3 provides an explanation for the larger than expected variation among migrant-pool metapopulations (fig. 4.6 right). Individual-based simulations predict maximum differentiation among the metapopulations over time in the presence of local extinction. This suggests that due to the extinction/colonization dynamics, the original variation within demes is redistributed not only to variation among demes, but eventually to variation among metapopulations.

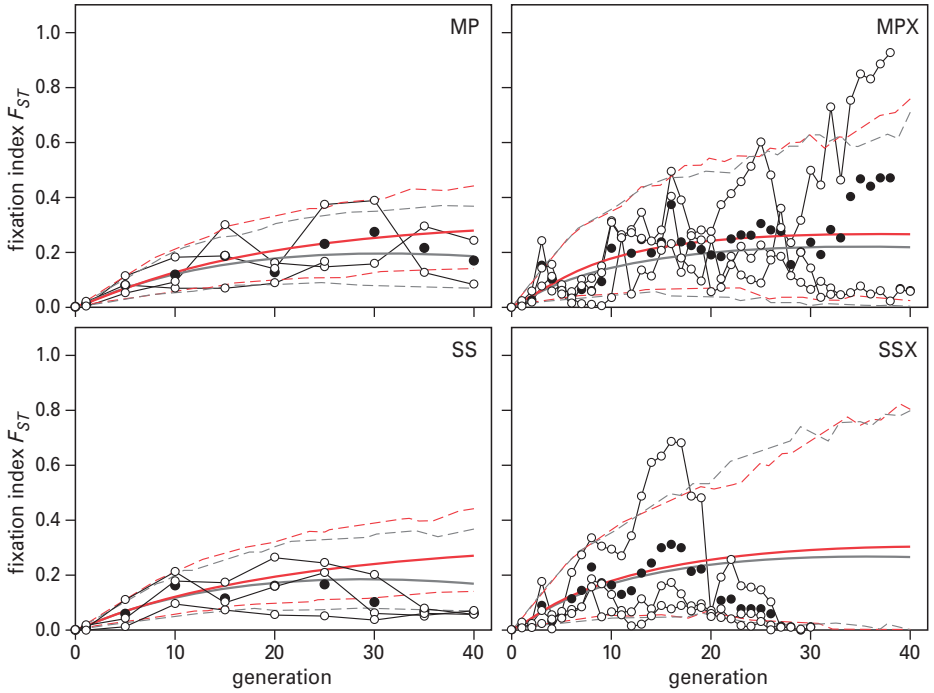

Figure 4.6. Observed and predicted genetic differentiation in metapopulations with migrant-pool (top) and stepping-stone (bottom) migration, in the absence (left) or presence (right) of local extinction and recolonization. The plots show the fixation index F_{ST} with symbols as in fig. 4.5. F_{ST}-series ending before generation 40 are due to allele fixation at the metapopulation level, so that the fixation index is no longer defined.

METAPOPULATION FITNESS AND STRESS TOLERANCE

In this section we investigate the effects of fragmentation and population turnover on the average fitness of our experimental metapopulations and their potential to cope with environmental challenges. In generation 35, we exposed flies from all demes and undivided populations to three environmental stress factors high (29°C) temperature, high (12.5%) ethanol concentration, and starvation. Figure 4.7 shows the results of the fitness assessments, while table 4.2 summarizes the results of the stress tolerance assessments.

Fragmentation in either the presence or absence of population turnover had a markedly different effect on fecundity (fig. 4.7 top) than on viability (middle). The variation in fecundity is relatively large both within (left) and among (right) metapopulations. The average fecundity is significantly lower in the metapopulations (Kruskal-Wallis $H = 11.5$, $df = 17$, $P = 0.0032$) than in the undivided bottle populations (right, white bar). In contrast, the viability at 25°C differs little both within (left) and among (right) metapopulations, and neither is it significantly different from the viability of the bottle populations (right, white bar). These results are most likely a consequence of the difference between vial and bottle populations in the experimental setup rather than of

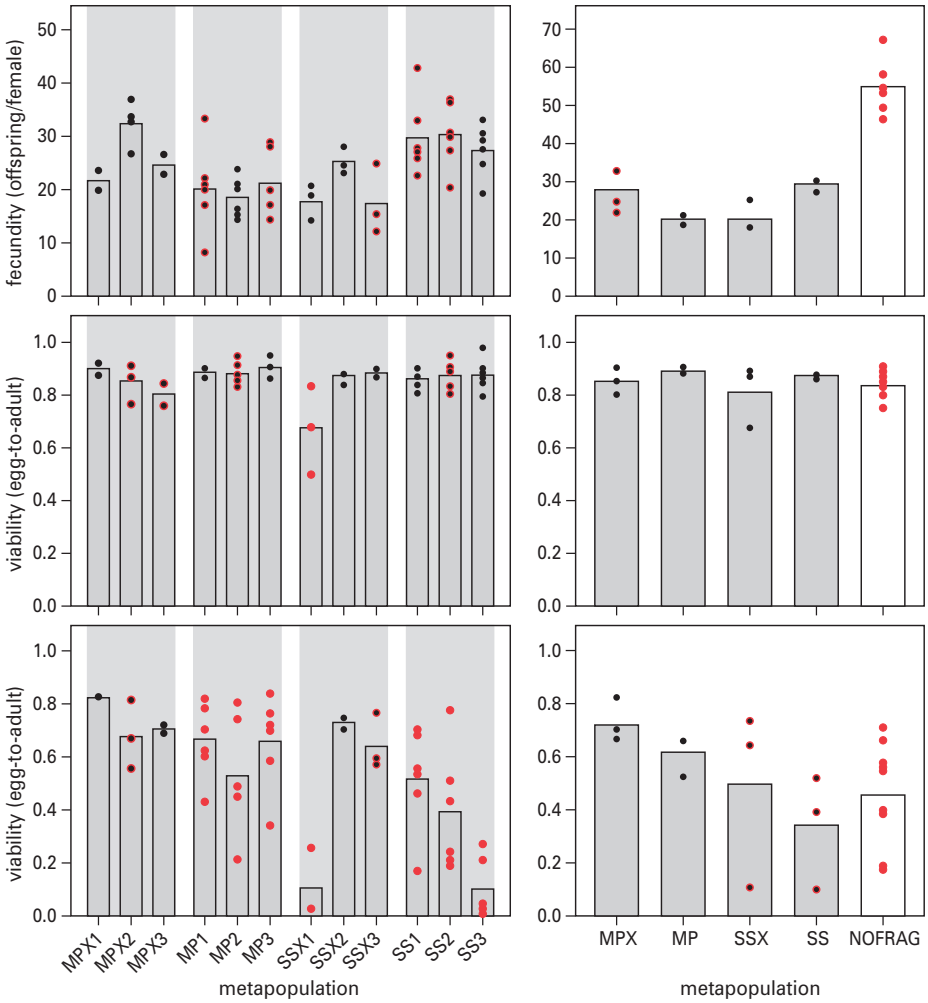

Figure 4.7. Fecundity (top) and viability at 25°C (middle) and 29°C (bottom) of experimental metapopulations with migrant-pool (MPX & MP) and stepping-stone (SSX & SS) migration. Left: average per metapopulation (bars) and values per deme (dots) for migrant-pool and stepping-stone migration in the absence and presence of local extinction. Right: average per migration/extinction scenario (bars) and per replicate metapopulation (dots). Note that the dots in the right-hand plots correspond to the bars in the left-hand plots. The white bars represent the undivided bottle populations. Dot colours indicate the level of significance of ANOVA among demes within metapopulations (left) and among metapopulations within scenarios (right). Black: $p \geq 0.05$, grey with black outline: $0.01 \leq p < 0.05$, and grey: $p < 0.01$.

genetic erosion due to population fragmentation We will discuss this further in the next section. The near maximal and very similar levels of viability of both metapopulations and bottle populations suggest that inbreeding depression plays no important role in any of the migration/extinction scenarios, although single demes might suffer from inbreeding depression to some extent, *e.g.*, in SSX1 (fig. 4.7 middle left).

The bottom plots in figure 4.7 show the egg-to-adult viability at 29°C. Exposure to high temperature reduces the viability in all scenarios, and substantially increases the variation, both within (left) and among (right) metapopulations and bottle populations. Upon visual inspection one might conclude that differences between the scenarios exist. However, none of these differences is statistically significant, and moreover, they do not represent a systematic trend. The tolerance (*i.e.*, relative viability) to high temperature stress (table 4.2) matches the pattern of the viability at 29°C very closely, since the viability under control conditions at 25°C is nearly constant. The results for the tolerance to ethanol stress and starvation resistance show similar, but less pronounced patterns of variation (tab. 4.2). The different tolerance patterns for high temperature and for high ethanol concentrations might partially result from the different genetic bases of both factors (CHAPTER 5). Although tolerance to high temperature is thought to be mostly a polygenic character (Loeschcke *et al.* 1997), conditionally expressed near-lethal alleles occur regularly for this trait (Bijlsma *et al.* 1999, Vermeulen & Bijlsma 2004). Such alleles behave like near-neutral alleles under normal conditions, hence they are merely subject to genetic drift and may show considerable variation in frequency in small populations. This is consistent with the observed high variation in tolerance both within (fig. 4.7 left)

Table 4.2. Stress tolerance in experimental metapopulations with migrant-pool (top, MPX & MP) and stepping-stone (bottom, SSX & SS) migration. Stress tolerance is the egg-to-adult viability under stress conditions relative to the viability under control conditions, and starvation resistance is the median age at death (in hours) of virgin males on agar medium. All averages are arithmetic means with standard errors in brackets.

metapopulation	tolerance to temperature stress	tolerance to ethanol stress	starvation resistance
MPX1	0.918 (0.021)	0.655 (0.001)	115.3 (1.8)
MPX2	0.793 (0.059)	0.782 (0.008)	120.4 (2.6)
MPX3	0.882 (0.065)	0.696 (0.018)	135.3 (10.3)
MP1	0.745 (0.062)	0.818 (0.035)	129.0 (3.2)
MP2	0.600 (0.107)	0.749 (0.036)	129.8 (5.5)
MP3	0.725 (0.076)	0.735 (0.023)	128.2 (2.4)
MPX	0.864 (0.014)	0.711 (0.005)	123.6 (2.7)
MP	0.690 (0.013)	0.767 (0.004)	129.0 (0.9)
SSX1	0.127 (0.090)	0.449 (0.044)	122.0 (0.6)
SSX2	0.841 (0.030)	0.641 (0.060)	119.7 (2.7)
SSX3	0.724 (0.066)	0.780 (0.048)	134.9 (3.8)
SS1	0.605 (0.096)	0.725 (0.057)	123.0 (3.4)
SS2	0.453 (0.112)	0.631 (0.040)	124.4 (2.3)
SS3	0.116 (0.054)	0.573 (0.037)	128.1 (1.4)
SSX	0.564 (0.017)	0.623 (0.005)	125.5 (0.9)
SS	0.392 (0.017)	0.643 (0.006)	125.2 (0.6)
Control bottles[1]	0.540 (0.062)	0.633 (0.032)	132.8 (1.9)

[1]) All measures were calculated for control bottles 1 – 12, but without the data of bottle 7

and among (right) metapopulations. Founder events involving very few individuals may enhance the effect of genetic drift, leading to the near-fixation of either allele at the metapopulation level. In line with this reasoning, we observe less variation among demes in the presence of local extinction (fig. 4.7 left, series MPX and SSX). However, entire metapopulations may become very susceptible to adverse external conditions, as has clearly happened in two of the experimental metapopulations (fig. 4.7 left, SSX1 and SS3). Tolerance to ethanol is mostly determined by a major gene (ADH), with other genes playing additional roles (Chakir *et al.* 1996, Malherbe *et al.* 2005). Analysis of the ADH locus (data not shown) has shown that both alleles ADH-F and ADH-S were initially present at frequencies of 0.44 and 0.56, respectively. During the experiment, selection in favour of the ADH-S allele has occurred in most metapopulations, increasing its frequency up to 1.0, *i.e.*, fixation, on three occasions. These results are somewhat atypical, since the equilibrium frequency of ADH-S in laboratory stocks under standard conditions generally varies between 0.25 and 0.35, whereas high concentrations ethanol induce selection in favour of ADH-F (Van Delden *et al.* 1978). Although one might expect a low tolerance of ethanol stress in populations with a high ADH-S frequency, we observed no correlation at all. We suspect that the ethanol concentrations in the experimental setup were too low to affect viability very much, so that the observed results reflect some other aspect of survival that is probably not connected with tolerance to ethanol at all (see *e.g.*, Bijlsma-Meeles & Bijlsma 1988).

DISCUSSION

EXPERIMENTAL SETUP

We have chosen initial experimental values that allow for ample population turnover with a colonization rate equal to the extinction rate. In such systems we expect the turnover rate of empty and extant demes to maintain viable metapopulations when the number of demes is sufficiently large. The experimental metapopulations, however, did not stabilize and would have gone extinct eventually in most cases. In addition to the cost of migration that negatively affected the turnover rate in the migrant-pool setup, this is probably a consequence of two important deviations between the experimental setup and theoretical assumptions. Firstly, theoretical models generally assume no demography within demes and instant growth to the maximum deme size after colonization, resulting in equal contributions to the next generation for each deme. The observed deme size after colonization ranged from 5 to 108 individuals (38 on average), hence it took two or more generations to attain maximum size on several occasions. We found similar large fluctuations in the size of extant demes, albeit with a higher average, implying that the contribution per generation may have varied considerably for the experimental demes. Secondly, the experimental migration, extinction and colonization rates fluctuated due to large variation in migration activity between generations, whereas these parameters are generally assumed constant in the theoretical models. This applies in particular to the assumption of colonization occurring instantly after extinction,

whereas effective migration, and thus, colonization, was (much) lower than the extinction rate in most experimental metapopulations. In retrospect, migration rates should probably have been planned twice as high, since on average, half of the migrants are males that will commonly contribute to gene flow when they immigrate into extant demes, but not when they colonize empty demes where no females are present. Fluctuations of these parameters have probably substantially increased the variation in the experimental systems, and thus, the risk of stochastic metapopulation extinction. Although we allowed for "natural" migration behaviour within the constraints of the spatial setup and for fluctuating deme sizes on purpose assuming only small differences averaging out within a few generations, these results show that relaxing experimental control to a little extent might easily result in large deviations from predictions based on theoretical models.

We hypothesized earlier that some of the differences between the metapopulations and the bottle populations were probably partly a consequence of the experimental setup. We suspect that even under relatively simple standard conditions, unintentional differences have been more common than expected, *e.g.*, between the vial and bottle populations. Due to the different experimental procedure for both types of containers, the population density in the bottles was generally higher than in the vials. Different densities might *e.g.*, introduce selection on the timing of egg-laying favouring early-laying females in the bottles (see fig. 4.7), resulting in a higher fecundity in the bottles, but not affecting egg-to-adult viability. Such unintentional density-dependant selection effects might provide an explanation for the difference between metapopulations and undivided populations that we found for fecundity, but not for viability. A second example of unforeseen differences is the cost of migration that we encountered in the migrant-pool configuration. The occurrence of such relatively large biases under simple standard conditions strongly suggests that many more unknown deviations of the model assumptions can be expected in natural metapopulations.

We observed (very) high levels of variation among single replicates for all migration and gene flow scenarios. Although such high variation is not unexpected, especially in the presence of population turnover, we suspect that part of the variation is due to the logistic constraints of the experimental setup, *i.e.*, the combination of few replicates, few demes per metapopulation, and using a single marker locus. We used simulations to evaluate the effect of these factors by varying the numbers of demes and marker loci, and averaging over a large number of replicate runs. Figure 4.8 compares the median and the 75%, 90% and 95% confidence intervals for the genetic differentiation in generation 40 based on individual-based simulations of a migrant-pool metapopulation consisting of six (left) or 60 (right) demes for one locus and for eight loci. Increasing either the number of demes or the number of marker loci reduces the width of the confidence intervals, and hence the variation, in both gene flow scenarios. In the presence of local extinction, however, the medians for small and large metapopulations differ considerably for both sets of marker loci, indicating a genuine consequence of metapopulation size rather than merely a sampling effect. Consequently, extrapolation of our experimental results based on metapopulations consisting of only a few demes to larger systems must be considered with care, and has probably limited value.

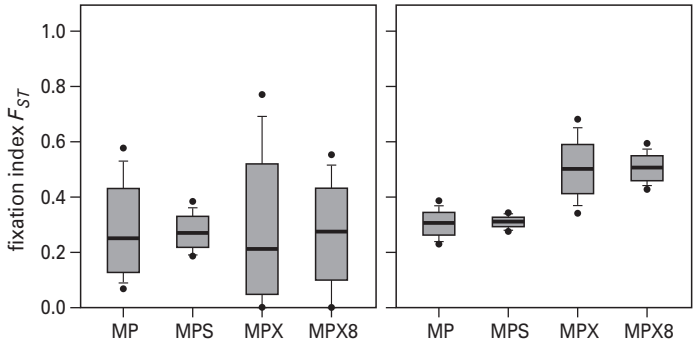

Figure 4.8. Predicted variation in genetic differentiation in a metapopulation consisting of few (left, $n = 6$) and many (right, $n = 60$) demes for a single locus and for multiple loci. The plots show the results of individual-based simulations without selection of 1000 replicate metapopulations with migrant-pool migration in the absence (MP) and presence (MPX) of local extinction and recolonization. Bars, whiskers and points indicate the 75%, 90% and 95% confidence intervals, respectively, for F_{ST} at one locus (MP, MPX) and averaged over eight loci (MP8, MPX8) in generation 40. The black bands in the bars indicate the median.

IMPLICATIONS FOR NATURAL SYSTEMS

We found clear deviations between the experimental results and theoretical predictions. Firstly, individual-based simulation predicted similar dynamics for migrant-pool and stepping-stone migration, whereas the observed patterns were different for both configurations. Secondly, the loss of genetic diversity proceeded generally more rapidly than predicted, resulting in allele fixation at the metapopulation level. Thirdly, the variation between replicate metapopulations was larger than expected in most cases. We can suggest several potential causes that may be responsible for these deviations. Most obviously, the actual migration rates were highly variable over generations, which had different consequences for each of the metapopulations, since the number of empty demes also differed over generations, and a low migration rate will have considerably less impact for extant demes than for empty demes. In addition, the physical dispersal distance was different for the two migration configurations, which unintentionally introduced an extra cost of migration in case of migrant-pool migration. Although variation at the eye colour marker locus was presumed to be neutral (Buri 1956), it was actually subject to selection, probably for subtle reasons such as different activity patterns due to the experimental light regime. In addition, the strength of selection was different in the vials than in the bottles (CHAPTER 2). Small differences in the experimental conditions in both types of container, such as occasional moderate crowding in the bottles, might have resulted in different selection pressures affecting fecundity, and thus the assessment of fitness. Finally, due to the different extinction schedules for each replicate metapopulation chance has played a very important role, which resulted in each replicate being unique and making general inferences difficult. All these factors will to some extent lead to deviations between the experimental results and theoretical predictions. We can

minimize such deviations by further standardization, *e.g.*, by replacing bottle populations with compound vial populations. However, one might argue that fully standardized experiments have limited use, because corresponding results are much easier obtained by simulations. In contrast, less-standardized experiments provide a bridge between theory and the natural world because they draw attention to subtle but important deviations that induce a better understanding of natural populations. Large variation in a relatively standardized setup indicates that even more variation can be expected in natural systems.

Since theoretical models, and also generalized simulation models, are primarily conceptual models providing general insights, it is unclear whether they have predictive value for natural populations that have all specific characteristics. In practice, one might ask how well measures of F_{ST} and n from natural populations are suited to make inferences of *e.g.*, effective metapopulation sizes based on a general model making many restricting assumptions as in equations (4.1) and (4.2). With $N_e = 28$, $m = 0.02$ and $e = 0.1$, we would expect $\hat{F}_{ST}$ (eqn (4.1)) to vary between $\hat{F}_{ST} = 0.27$ for metapopulations with local extinction and migrant-pool colonization ($\varphi = 0$), and $\hat{F}_{ST} = 0.31$ in the absence of extinction. The results in fig. 4.6 suggest that the experimental populations did not attain equilibrium levels of F_{ST} in most cases, since F_{ST} dropped sharply after 20 to 25 generations due to allele fixation in the metapopulations, whereas the simulation results (red lines) indicate that it will generally take longer than 40 generations to attain equilibrium. In addition, the number of $n = 6$ demes in our metapopulations is below the limit of $n = 20$ that is considered sufficiently large to approximate the equilibrium in a model II metapopulation with the model I equation (Pannell & Charlesworth 1999), although simulations (data not shown) indicate that the equilibrium in a model II metapopulation with six demes is only marginally lower than the approximation based on eqn (4.1). Hence, the experimental F_{ST}-values in generation 20 that we used to infer effective metapopulation sizes are probably lower than the actual equilibrium values.

The effective size of a metapopulation is a measure of the loss of genetic variation from the metapopulation. In the experimental metapopulations, the genetic variation within demes decreased, whereas the variation among demes increased initially to drop again as most metapopulations lost all variation due to allele fixation. Estimates of the effective metapopulation size N_e^M based on the generalised model in eqn (4.2) are independent of spatial structure, but depend directly on F_{ST}. Subject to a number of assumptions, table 4.3 shows the estimated N_e^M averaged over the three replicate experimental metapopulations per scenario (col. 2). In the absence of population turnover, the estimated effective size of the metapopulations is larger than the predicted effective size ($N_e = 168$) of an undivided population of equal total size ($N = 6 \times 50 = 300$). Due to local extinction and recolonization, the estimated effective metapopulation size is drastically reduced in comparison with an undivided population. These results are in general accordance with theoretical predictions (Wang & Caballero 1999), but it is unclear whether such estimated values are reliable as absolute quantities.

Equation (4.2) allows for some deviation of its assumptions, for example by using the effective deme size instead of the census deme size to correct for non-random mating within demes. Likewise, using F_{ST} may allow for the presence of directional selection to

Table 4.3. Effective metapopulation size N_e^M for metapopulations with migrant-pool (top) and stepping-stone (bottom) migration, in the absence (MP, SS) or presence (MPX, SSX) of local extinction and recolonization. Column 2 shows the estimated effective size of three replicate metapopulations based on the average F_{ST} in generation 20 (the range of single replicates in brackets). Columns 3 and 4 show the variance and eigenvalue effective metapopulation sizes inferred from linear regression over 20 generations (see text). Values in italics are corresponding results of individual-based simulations of 1000 replicate metapopulations (95% confidence intervals in brackets).

metapopulation	F_{ST}-based N_e^M	variance N_e^M	eigenvalue N_e^M
MPX	62.1 (19.3 – 85.5)	528.7 (386.0 – ∞)	43.3 (18.8 – 422.2)
MP	192.0 (183.6 – 198.9)	33.3 (16.4 –132.2)	14.4 (7.8 – 126.0)
MPX sim	*43.3 (37.0 – 109.9)*	*34.9 (31.7 – 39.0)*	*34.9 (29.0 – 43.8)*
MP sim	*210.8 (185.4 – 250.7)*	*203.3 (194.7 – 212.7)*	*188.7 (175.0 – 204.7)*
SSX	93.6 (67.6 – 89.6)	320.0 (164.9 – ∞)	9.3 (7.0 – 12.4)
SS	199.6 (178.0 – 228.3)	62.7 (24.7 – ∞)	33.8 (17.4 – ∞)
SSX sim	*43.8 (38.6 – 117.7)*	*32.9 (30.1 – 36.1)*	*37.5 (31.3 – 46.9)*
SS sim	*208.0 (184.9 – 246.5)*	*199.5 (190.5 – 209.3)*	*176.3 (156.4 – 202.1)*

some extent, because the effects of selection are reflected in the fixation index. However, other simplifying assumptions, for example regarding the variance of reproductive output among demes, might considerably affect estimates of the effective metapopulation size. We expect that the variance of reproductive output among demes is larger than predicted in the experimental metapopulations, since the observed fluctuations in the migration, colonization and extinction rates, as well as in deme size and in the number of extant demes all affect the reproductive output of demes. Inspection of the observed variance (tab. 4.3, col. 3) and eigenvalue (col. 4) effective sizes attracts immediate attention to the striking discrepancies between both concepts of effective size, pointing out that the theoretical approximation obviously does not hold in the presence of natural selection. Comparison of the estimator based on F_{ST} and the variance and eigenvalue effective sizes based on idealized simulated populations without selection (tab. 4.3) suggests that the F_{ST}-based estimator is fairly robust in the absence of population turnover, but inclined to substantial discrepancies (up to 50%) when local extinction and recolonization events occur frequently. Its value for applied studies where the effective metapopulation size is used as an indicator of for instance the risk of inbreeding depression in a population might therefore be limited in practice.

ACKNOWLEDGEMENTS We thank M.H. Edelenbos, A. Boerema, L. Hoeksema and A. Rumahloine for their technical assistance. This project was financially supported by the Netherlands Foundation for the Advancement of Tropical Research (WOTRO), as part of the Priority Program "Biodiversity in Disturbed Ecosystems" of the Netherlands Organization for Scientific Research (NWO).